Geomechanics and Engineering, *Vol. 27, No. 2 (2021) 179-187*
https://doi.org/10.12989/gae.2021.27.2.179

Applicability of liquid air as novel cryogenic refrigerant for subsea tunnelling construction

Youngjin Son[1a], Tae Young Ko[2b], Dongseop Lee[3], Jongmuk Won[4], In-Mo Lee[5] and Hangseok Choi*[5]

[1]Eco Infra Solutions Team2, SK Ecoplant, Seoul, 03149, Republic of Korea
[2]Department of Energy and Resources Engineering, Kangwon National University, Kangwon, 24341, Republic of Korea
[3]POSCO, Incheon, 21998, Republic of Korea
[4]Department of Civil Engineering, University of Ulsan, Ulsan, 44610, Republic of Korea
[5]School of Civil, Environmental, & Architectural Engineering, Korea University, Seoul, 02841, Republic of Korea

(Received July 21, 2020, Revised June 29, 2021, Accepted October 7, 2021)

Abstract. The artificial ground freezing technique has been widely adopted in tunnel construction in order to impede heavy water flow and to reinforce weak sections during excavation. While liquid nitrogen is one of common cryogenic refrigerants particularly for rapid freezing, it has a serious potential risk of suffocation due to an abrupt increase in nitrogen content in the atmosphere after being vaporized. This paper introduces a novel cryogenic refrigerant, liquid air, and addresses the applicability of it by performing a series of laboratory chamber experiments. The key parameters for the application of artificial freezing using liquid air in subsea tunnel construction are freezing time and energy consumption, which were evaluated and discussed in this paper. The comparative study of these parameters between the use of liquid air and liquid nitrogen demonstrates that liquid air with no risk of suffocation can be a potential substitute for liquid nitrogen delivering the equivalent performance. In addition, the theoretical model was adopted to evaluate the chamber experiments in an effort to estimate the freezing time and the energy consumption ratio (energy consumption for maintaining the frozen state to the energy consumption for freezing soil specimens).

Keywords: artificial ground freezing; energy consumption ratio; freezing time; heat transfer; liquid air; refrigerant

1. Introduction

Subsea tunnels are vulnerable to seawater intrusion caused by unpredictable high-water pressure during construction, which necessitates substantial ground improvement in order to prevent potential risky incidents. Conventional grouting methods (e.g., jet grouting, permeation grouting and compaction grouting) may not be applicable to subsea tunnel construction because high pore-water pressure inhibits grouting materials to penetrate deep enough to increase the strength of soil. Some case studies have been reported on utilization of the freezing technique in the subsea tunnel (Zhang *et al*. 2014), it is still questionable that this technique is applicable to all types of soil. Therefore, the artificial ground freezing technique can be adopted as an alternative ground improvement method, which is environmentally friendly and applicable to most soil types (Andersland and Ladanyi 2004).

In spite of pronounced advantages of the artificial ground freezing technique, the application of this technique can be restricted particularly in enclosed space during construction of relatively long tunnels. In addition, the economical aspect of energy supply for maintaining frozen soil has not been investigated yet. While an extensive body of research has been performed for investigating the fundamental behavior of frozen soils (Li *et al*. 2011, Yang *et al*. 2010a, Yang *et al*. 2010b), few studies have been conducted to apply the artificial ground freezing technique to subsea tunnel construction.

Liquid nitrogen and brine are the two most common refrigerants that have been widely adopted for ground freezing applications (Pimentel *et al*. 2012, Vitel *et al*. 2015). Even though liquid nitrogen has an advantage of having short freezing time along with the extremely low boiling temperature, a critical safety issue (i.e., suffocation of workers) arises when using this technique in enclosed construction environment such as a long-span subsea tunnel. In contrast, using brine has no issue related to suffocation, it requires a relatively high initial installation cost of freezing facilities including refrigerant plants. Thus, the combined method (liquid nitrogen + brine) has been occasionally used in case of adverse construction conditions (Gallavresi 1981).

This paper presents a novel cryogenic refrigerant, i.e., liquid air, for ground freezing in order to eliminate the potential risk of suffocation of workers in enclosed space. Liquid air, produced by mixing liquid oxygen and liquid nitrogen, was produced in the laboratory under three different mixing ratios. The feasibility of liquid air as a potential refrigerant was assessed by performing a series of chamber experiments designed for freezing soil specimens.

*Corresponding author, Professor, Ph.D.
E-mail: hcchoi2@korea.ac.kr
[a]General Manager, Ph.D.
E-mail: sohnyjin@daum.net
[b]Assistant Professor, Ph.D.
E-mail: tyko@kangwon.ac.kr

ISSN: 2005-307X (Print), 2092-6219 (Online)

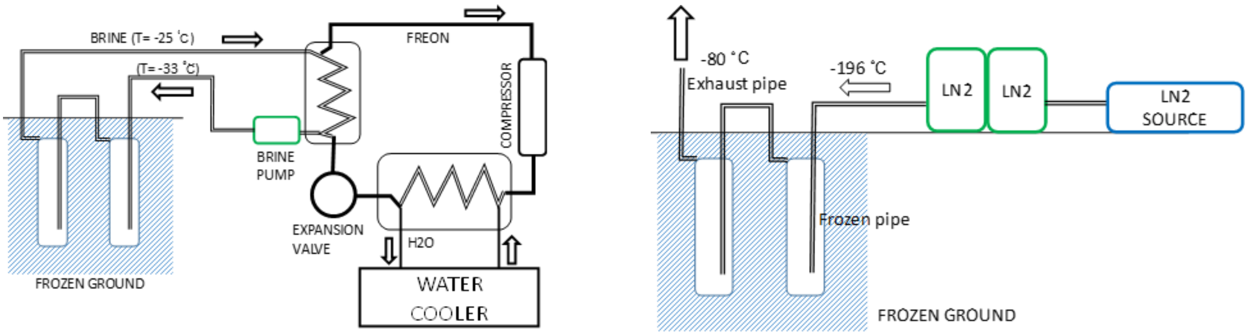

(a) With brine (b) With liquid nitrogen

Fig. 1 Schematic diagram of ground freezing methods using brine and liquid nitrogen (Colombo *et al*. 2008)

Table 1 Characteristics of refrigerants (from Stoss and Valk 1979)

	Brine	Liquid nitrogen	Liquid air
Minimum temperature	-55~-34°C *	-195.8 °C *	-194.5 °C *
Application section	open and enclosed	open space	open and enclosed
Reused of coolant	standard	impracticable	impracticable
Frost penetration	slow	fast	fast
Toxicity	small	required ventilation	none
Refrigeration plant	required	not required	not required

* Theoretical value

The theoretical model was also presented, which can be used to estimate the freezing time and energy consumption ratio.

2. Refrigerants for artificial ground freezing

Brine has been widely used as a secondary refrigerant in tunnel construction because it is inexpensive by recycling the refrigerant and stable with no risk of suffocation of workers (Backer and Blindheim 1999, Haβ and Schäfers 2005, Heijboer *et al*. 2003, Pimentel *et al.* 2011, Saarelainen *et al*. 2004, Wang *et al.* 2016, Wang *et al.* 2018, Wang *et al.* 2019). However, the use of brine takes relatively long freezing time and requires a high initial installation cost for cooling and circulating brine in refrigerant plants as illustrated in Fig. 1(a). In general, brine is normally adopted as a refrigerant under the groundwater velocity less than 2 m / day, for the target freezing volume ranging from 200 to 35,000 m^3, which demands the freezing time of 3 to 12 weeks (Harris,1995).

The use of liquid nitrogen in artificial ground freezing expedites the freezing process by injecting liquid nitrogen with extremely low temperature ranging from -210.0°C to -195.8°C in a liquid phase (Cai *et al*. 2020, Evirgen and Tuncan 2019, Itoh *et al*. 2005, Mauro *et al*. 2020, Pimentel *et al*. 2012). This freezing technique has advantages of the simple installation of freezing facilities (Fig. 1(b)) and the ability to achieve a strengthened frozen body in a very short time. However, unlike brine, liquid nitrogen cannot be recycled, and the vaporized nitrogen substantially increases nitrogen concentration, which causes a potential risk of suffocating workers near exhaust pipes. Liquid nitrogen is generally adopted as a refrigerant under the groundwater velocity greater than 2 m / day and less than 20 m / day, for the target freezing volume of about 200 m^3, which demands the freezing time less than 1 week.

As mentioned above, the use of liquid nitrogen leads to a critical safety issue that the vaporized nitrogen can suffocate the workers particularly in enclosed space. Such fatal weakness lessens the applicability of liquid nitrogen as a cryogenic refrigerant. To eliminate this potential risk of suffocation, liquid air was considered as a new refrigerant for ground freezing, and its performance was evaluated in this paper. The composition of liquid air is analogous to that of air in the atmosphere, and thus the potential risk of suffocation can be dramatically reduced when liquid air is vaporized. Because the boiling point of liquid air (-194.5°C) is as low as that of liquid nitrogen (-195.8°C), the use of liquid air also provides rapid ground freezing as liquid nitrogen does. Table 1 summarizes the characteristics of three refrigerants mentioned above.

3. Refrigerants for artificial ground freezing

3.1 Liquid air production system

Contrary to liquid nitrogen or liquid oxygen, liquid air is not commercially available in the current manufacturing industry. Therefore, a mixing process of liquid nitrogen and liquid oxygen is required to produce liquid air. Because of a slight difference in the boiling points of liquid nitrogen (-195.8°C) and liquid oxygen (-182.95°C), heat exchange between the two liquids occurs until the mixed liquid reaches the thermodynamic equilibrium state (Giancoli 1984). This leads to partial evaporation of liquid nitrogen (due to heat transfer from liquid oxygen to liquid nitrogen) during the mixing process, and thus raises the initial ratio of liquid oxygen content to liquid nitrogen. Therefore, it is necessary to investigate the oxygen concentration in the atmosphere after liquid air is vaporized according to various mixing conditions in the mixing chamber such as the initial mixing ratio, vessel pressure and outflow rate of exhausted gas.

Fig. 2 Overview of apparatus for producing liquid air

Table 2 Physical properties of silica sand adopted in chamber experiment

Property	Value	Standard
d_{50} (mm)	0.5	ASTM C136
C_u	1.56	ASTM C136
e_{max}	1.03	ASTM D4253
e_{min}	0.64	ASTM D4254
G_s	2.64	ASTM D854

(a) Perspective view (b) Overview (c) Thermocouple Points

Fig. 3 Perspective view and picture of designed freezing chamber

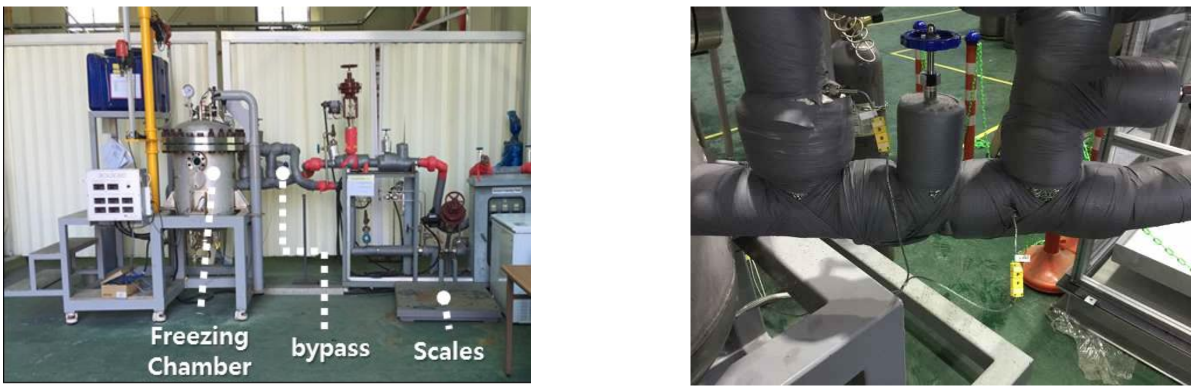

(a) Experimental setup (b) Insulated bypass pipes

Fig. 4 Overview of lab-scale freezing chamber test

The oxygen concentration of exhausted air from the mixing chamber was monitored for several hours by the oxygen sensor with the measurement error of ±1% and range of 0 ~ 30%. Considering the standard oxygen concentration of 18.0 ~ 23.5% specified by the Korean Occupation Safety and Health Acts, the target oxygen concentration of liquid air was set to 19.0 ~ 23.0% in this paper. In addition, XL-45 gas cylinders (508 mm in diameter and 1,562 mm in height) were used to mix liquid nitrogen with liquid oxygen and to store the produced liquid air. Fig. 2 shows the overview of producing liquid air. The experimental procedure is summarized as follows: (a) careful inspection of all equipment to prevent any potential malfunctioning (valves, scales, flow meter, pressure sensors, etc.), (b) cleansing all the pipes using liquid nitrogen, (c) cooling down all the pipes until the temperature reaches -190°C, (d) zeroing the scales, (e) supplying the target amount of liquid nitrogen into the mixing chamber, (f) supplying the target amount of liquid oxygen into the mixing chamber, (g) controlling the pressure and outflow rate in the mixing chamber and (h) data acquisition.

3.2 Lab-scale freezing chamber experiment

In order to assess the applicability of liquid air as a cryogenic refrigerant in subsea tunnel construction, a lab-scale freezing chamber was designed to performing a series of artificial freezing experiments. Salinity was considered as an influential factor governing the freezing time for saturated soils, which represents the chemical composition of subsea pore- water. Liquid nitrogen and liquid air were comparatively used as refrigerants in freezing silica-sand specimens. Physical properties of the fairly-uniform silica sand is summarized in Table 2.

The dimension of the cylindrical freezing chamber was determined by considering two factors: 1) the diameter of the freezing pipe where refrigerants such as liquid nitrogen can be injected without clogging, and the vaporized gas can be freely discharged, and 2) sufficient clearance was secured to minimize the effect of ambient temperature. The cylindrical freezing chamber was made of stainless steel with the inner diameter of 584.2 mm as shown in Fig. 3. The pressure gauge and the safety valve were placed at the top cap of the chamber, and the water supply valve was equipped at the bottom part of the chamber for saturating the soil specimen. The refrigerant (i.e., liquid nitrogen or liquid air) was supplied through a flexible pipe, which is connected to the freezing pipe embedded at the center of the soil specimen. All the pipes were surrounded by polyurethane foam (Fig. 4(b)) in order to insulate liquid nitrogen and liquid air from the ambient temperature.

The freezing pipe was designed as a coaxial pipe, which allowed circulation of the refrigerant from the inner pipe to the outer pipe (i.e., the liquid refrigerant was supplied through the inner pipe and discharged through the outer pipe). Four thermocouples were installed at every 51 mm from the freezing pipe in the radial direction (Fig. 3(c)) to monitor temperature with time and to estimate the freezing time at each location. All the monitored data such as the temperature and pressure inside the chamber are shown on the panel next to the chamber (the white box in Fig. 4(a)). Thermocouples were additionally installed on the inlet and outlet pipes. The procedure of chamber experiments performed in this paper was identical to the procedure of liquid air production from step (a) to (d). The following steps are as follows: (e) supplying the refrigerant, (f) controlling the pressure and flow rate in the chamber and (g) data acquisition. The freezing test was continued until temperature at the Point 4 thermocouple (204 mm away from the freezing pipe) became -2.0°C to prevent any severe damage to the chamber caused by considerable freezing expansion of the soil specimen. Four experimental conditions (Case 1~4) for the freezing chamber test are summarized in Table 3.

Table 3 Experimental cases considering types of refrigerants, salinity and conditions

Cases	Liquid Nitrogen		Liquid Air	
	Case 1	Case 2	Case 3	Case 4
Salinity	0‰	35‰	0‰	35‰
Temperature in chamber	16.0°C	17.9°C	7.1°C	5.5°C
Date	Apr. 23, 2015	May 13, 2015	Dec. 24, 2015	Dec. 22, 2015

3.3 Experimental results

3.3.1 Production of liquid air

The oxygen concentration measured in the gaseous air exhausted from the mixing chamber was continually monitored under the different mixing conditions in the mixing chamber such as the initial mixing ratio, vessel pressure and outflow rate of exhausted gas (refer to Fig. 5). The standard experiment case is that the initial mixing ratio of 80% (liquid nitrogen): 20% (liquid oxygen) on the basis of mol, the vessel pressure of 294.2 kPa and the outflow rate of 4.5 m^3 / hr at STP (0°C, 1 atm).

For all of three initial mixing ratios (that is, the ratio of liquid nitrogen to liquid oxygen = 75:25, 80:20 and 85:15 on the basis of mol), the measured oxygen concentrations in the gaseous air were slightly higher than the initial fraction of liquid oxygen. The mean oxygen concentration in the gaseous air was evaluated to be 28.28, 21.13 and 15.94% for the initial oxygen concentration of 25.0, 20.0 and 15.0%, respectively. Note that if the initial mixing ratio is 80:20, liquid air is vaporized to maintain the oxygen concentration of 18.2 ~ 21.6% in the gaseous air phase, which satisfies the standard of oxygen concentration of 18.0 ~ 23.5% (Korean Occupation Safety and Health Acts). Therefore, the target oxygen concentration of 19.0 ~ 23.0% in this paper can be obtained when applying the initial mixing ratio of 80:20.

The effect of pressure in the mixing chamber was investigated by setting the vessel pressure of 98.1, 294.2 and 490.3 kPa under the standard conditions with the mixing ratio of 80:20 and the outflow rate of 4.5 m^3 / hr at STP. The oxygen concentration of gaseous air exhausted from the mixing chamber was continually monitored. As

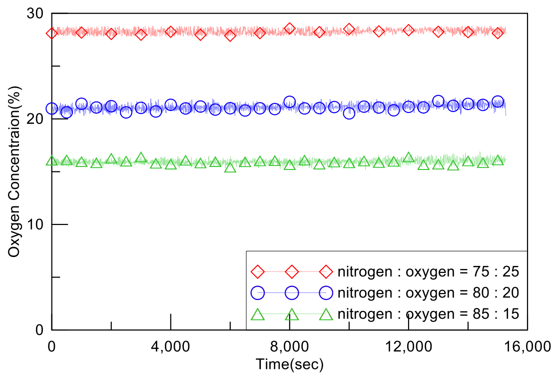

(a) Effect of initial mixing ratio

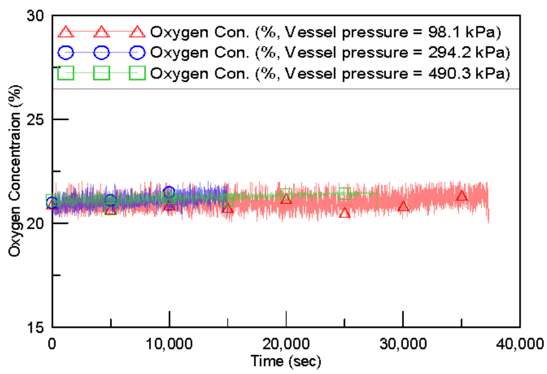

(b) Effect of vessel pressure

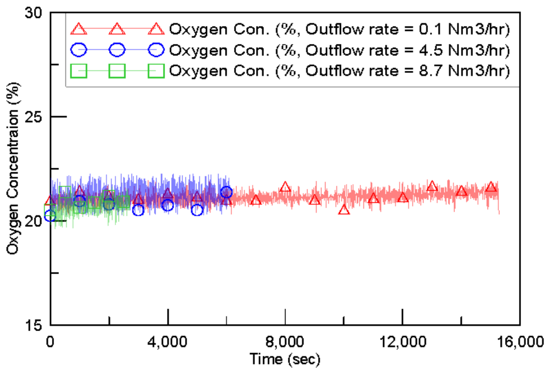

(c) Effect of outflow rate

Fig. 5 Comparison of oxygen concentration in gaseous air phase exhausted from mixing chamber

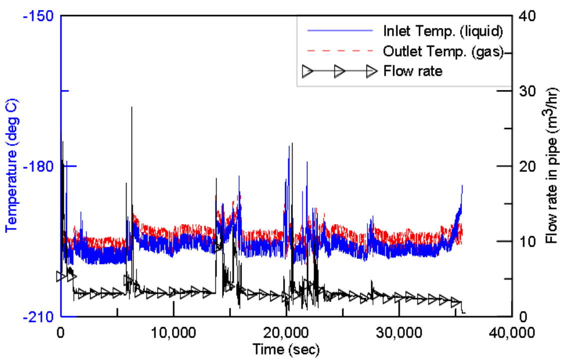

(a) Case 2

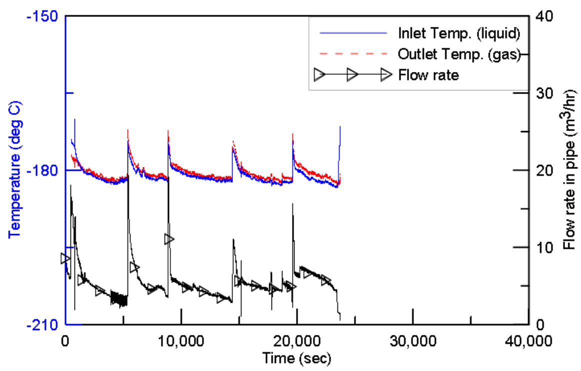

(b) Case 4

Fig. 6 The monitored temperature at inlet and outlet and flow rate in freezing pipe

seen in Fig. 5(b), the average oxygen concentration for the vessel pressure of 98.1, 294.2 and 490.3 kPa were evaluated to be 21.01, 21.13 and 21.24%. Even though slightly higher oxygen concentration was observed as the pressure increases, the effect of vessel pressure in the mixing chamber is not significant. An increase in the vessel pressure may result in an increase in the boiling point of liquid oxygen, and lead to a slightly larger amount of oxygen being vaporized. However, it is concluded that the oxygen concentration of gaseous air is not sensitive to the vessel pressure in the mixing chamber.

The effect of outflow rate of exhausted gas was investigated by setting the flow rate of 0.1, 4.5 and 8.7 m^3/hr at STP under the standard conditions with the mixing ratio of 80:20 and the vessel pressure of 294.2 kPa. As can be seen in Fig. 5(c), the oxygen concentration was also insensitive to the outflow rate of gaseous air and remained stable.

3.3.2 Lab-scale freezing chamber

The inlet and outlet temperature of the chamber and the flow rate of circulating refrigerant in the freezing pipe during the freezing process were monitored during the lab-scale freezing chamber tests. The use of liquid nitrogen (Case 2 in Table 3) and liquid air (Case 4 in Table 3) are compared in Fig. 6. The flow rate of injected liquid air was more than twice that of liquid nitrogen. Both the refrigerants showed that the measured outlet temperature was slightly higher than the inlet temperature throughout the freezing process because of heat exchange between the refrigerant and the soil specimen. An abrupt change in temperature and flow rate measurement is attributed to

Table 4 Results of freezing chamber test

Cases	Case 1	Case 2	Case 3	Case 4
	Liquid Nitrogen		Liquid Air	
Consumption (kgf)	397.3	381.2	426.5	364.7
Freezing time (hr)	9.37	8.94	5.88	4.97
Freezing temperature (°C)	0	-1.91	0	-1.91

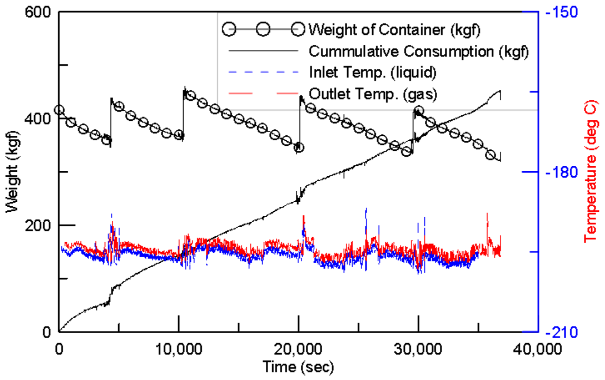

Fig. 7 Consumption of refrigerant (Case 1)

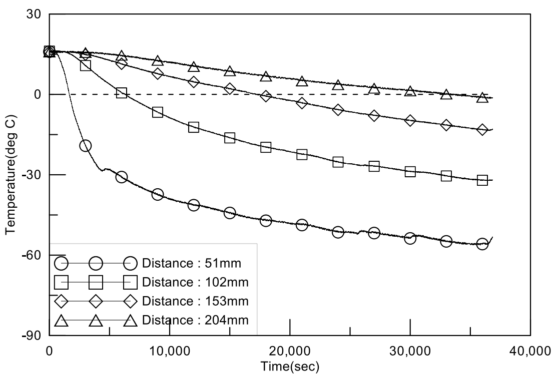

(a) Case 1

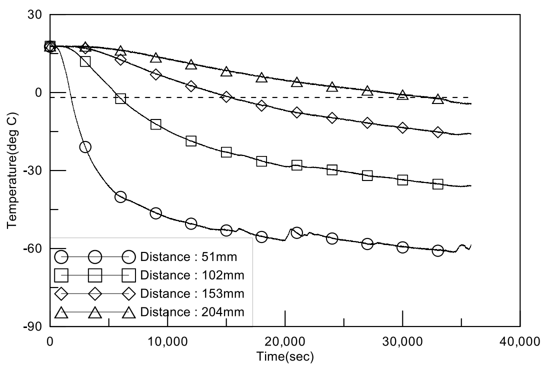

(b) Case 2

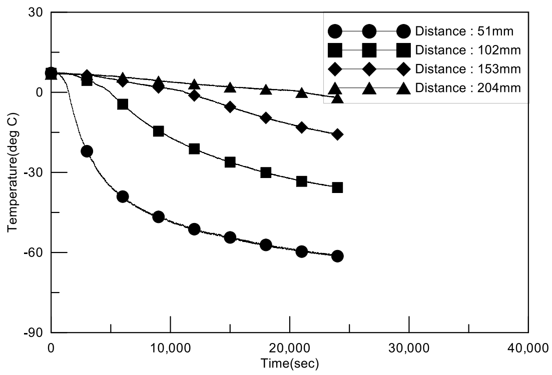

(c) Case 3

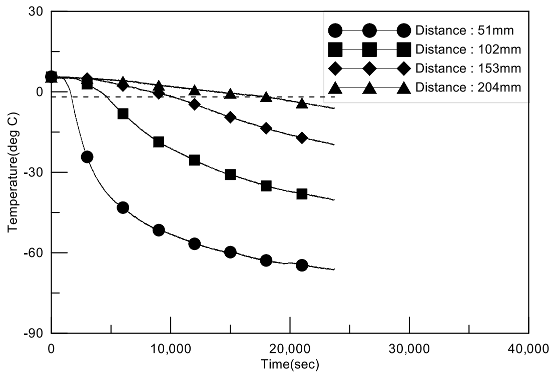

(d) Case 4

Fig. 8 Temperature in experiment over time at four thermocouples

replacing the depleted refrigerant container. Fig. 7 presents the consumption of liquid nitrogen (Case 1 in Table 3) along with the temperature data. The consumption of refrigerant was estimated by summing up the change in weight of the refrigerant container during the freezing chamber tests.

The total amount of consumed refrigerant, the freezing time at thermocouple Point 4 (204 mm away from the freezing pipe in Fig. 3(c)) and freezing temperature for Case 1 to 4 are summarized in Table 4. Because the chamber experiments using liquid air (Case 3 and 4) were performed in winter, the refrigerant consumption and freezing time show a favorable result compared to the cases of liquid nitrogen in this paper. Fig. 8 shows the temperature measurements with time at each location in the freezing specimen.

The freezing temperature of Case 2 and 4 was lower than that of Case 1 and 3 due to the effect of salinity (35‰) in pore-water. The required freezing time for both refrigerants decreased as salinity increased, which is presumably attributed to the higher thermal conductivity of frozen soil at the salinity of 35‰ compared to that of fresh water (i.e., salinity of 0‰). In order to prove this hypothesis, thermal conductivity of the unfrozen and frozen silica sand saturated with salty water (salinity of 35‰) and fresh water (salinity of 0‰) was measured by the transient hot wire method in the laboratory. In the case of unfrozen silica sand, the thermal conductivity for the salinity of 35‰ and 0‰ resulted in 2.2 and 2.1 W / m·K, respectively, which shows no significant difference. On the other hand, in the case of frozen silica sand, the thermal conductivity for the salinity of 35‰ and 0‰ resulted in 4.5 and 3.8 W / m·K, respectively. Consequently, it is concluded that the higher thermal conductivity of frozen soil saturated with salty water (salinity of 35‰) enhances heat transfer to reduce a total of freezing time in the freezing chamber test.

4. Evaluation of freezing time and energy consumption ratio

4.1 Theoretical model of heat flow Liquid air production system

Andersland and Ladanyi (2004) proposed a theoretical model to estimate radial temperature distribution from a single freezing pipe as schematically described in Fig. 9. Total heat energy for freezing soil up to the radius R consists of [1] the latent heat in the freezing zone, [2] the sensible heat induced by a difference in the freezing point between water and surrounding ground in the frozen zone,

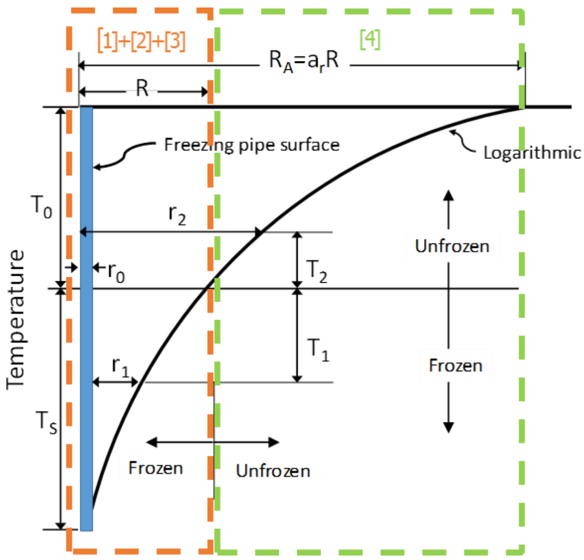

Fig. 9 Schematic description of temperature distribution from a single freezing pipe (Andersland and Ladanyi 2004)

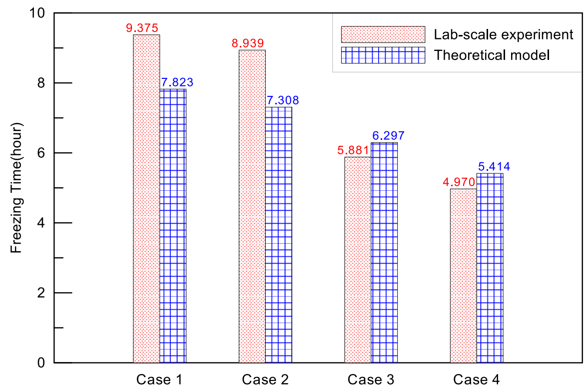

Fig. 10 Comparison of freezing time using lab-scale experiment and theoretical model

Table 5 Comparison of freezing performance estimated from theoretical model

Cases	Case 1	Case 2	Case 3	Case 4	Remarks
	Liquid Nitrogen		Liquid Air		
Energy consumption for freezing chamber specimen (MJ / m)	60.43	66.49	45.34	45.78	Eq. (1)
Freezing time at thermocouple Point 4 (hr)	7.82	7.31	6.30	5.41	Eq. (3)
Energy consumption for maintaining frozen state (MJ / m)	18.79	23.26	8.34	8.70	Eq. (4)
Energy consumption ratio	0.31	0.35	0.18	0.19	Eq. (4)/Eq. (1)

Note: Thermocouple Point 4 is located 204 mm away from the center of freezing pipe

[3] the sensible heat induced by a temperature difference between the freezing point of water and cooling temperature in the frozen area and [4] the sensible heat released into the unfrozen ground. The total heat energy can be calculated by Eq. (1), which is implemented to be Eq. (2). In addition, the freezing time is expressed as Eq. (3). Contrary to liquid nitrogen or liquid oxygen, liquid air is not commercially available in the current manufacturing industry. Therefore, a mixing process of liquid nitrogen and liquid oxygen.

$$Q=\pi R^2L+\pi R^2C_uT_o+\frac{2\pi C_fT_s}{\ln\frac{R}{r_o}}\int_{r_o}^{R}r_1\ln\frac{R}{r_1}dr_1+2C_uT_o\int_{R}^{a_rR}\left(1-\frac{\ln\frac{r_2}{R}}{\ln a_r}\right)r_2dr_2 \quad (1)$$

=[1] + [2] + [3] + [4]

$$Q=\pi R^2\left[L+\frac{a_r^2-1}{2\ln a_r}C_uT_o+\frac{C_fT_s}{2\ln\frac{R}{r_o}}\right] \quad (2)$$

$$t=\frac{R^2L_1}{4k_fT_s}\left(2\ln\frac{R}{r_o}-1+\frac{C_fT_s}{L_1}\right) \quad (3)$$

where R (m) is the radius to the frozen-unfrozen soil interface; L (J / m^3) is the volumetric latent heat of soil; $a_r = R_A/R$ (where R_A is the radius of temperature influence from the freezing pipe in the unfrozen soil); C_u (J / m^3·K) and C_f (J / m^3·K) are the volumetric heat capacity for the frozen and unfrozen soil, respectively; T_o (K) is a difference between the ambient ground temperature and the freezing point of water; T_S (K) is a difference between the freeze pipe surface temperature and the freezing point of water; r_o (m) is the radius of freezing pipe; k_f(W / m·K = J / m·K·hr) is the thermal conductivity of frozen soil.

The fourth term of Eq. (1), i.e., $Q_{[4]}$, is the sensible heat required to maintain the frozen state within the radius of R. In addition, $Q_{[4]}$ (J / m) can be expressed as Eq. (4) and indicates the amount of heat energy to maintain the frozen state at thermocouple Point 4 (204 mm away from the center) in the present chamber experiment.

$$
\begin{aligned}
Q_{[4]} &= 2\pi C_u T_o \int_R^{a_r R} \left(1 - \frac{\ln \frac{r_2}{R}}{\ln a_r} \right) r_2 dr_2 \\
&= 2\pi C_u T_o \left[\int_R^{a_r R} r_2 dr_2 - \frac{1}{\ln a_r} \int_R^{a_r R} \ln \frac{r_2}{R} r_2 dr \right] \quad if\ x = \frac{r_2}{R},\ r_2 = Rx,\ dr_2 = Rdx \\
&= 2\pi C_u T_o \left[\frac{1}{2} Rx^2 \Big|_1^{a_r} - \frac{1}{\ln a_r} \int_1^{a_r} \ln xRxRdx \right] \quad if\ R < Rx < a_r R \\
&= 2\pi C_u T_o \left[\frac{1}{2} R^2 \left(a_r^2 - 1 \right) - \frac{R^2}{\ln a_r} \int_1^{a_r} \ln x\ x\ dx \right] \\
&= 2\pi C_u T_o R^2 \left[\frac{1}{2} \left(a_r^2 - 1 \right) - \frac{1}{\ln a_r} \left\{ \frac{1}{2} a_r^2 \ln a_r - \frac{1}{4} \left(a_r^2 - 1 \right) \right\} \right] \\
&\therefore Q_{[4]} = \pi R^2 C_u T_o \left(\frac{a_r^2 - 1}{2 \ln a_r} - 1 \right)
\end{aligned}
\qquad (4)
$$

In this paper, the theoretical model was adopted to calculate the freezing time in the chamber experiment and the energy required to maintain the frozen state. The density of silica sand specimen in the chamber was measured to be 1,854 kg / m^3. The values of heat capacity for saturated and frozen samples were estimated based on the values of specific heat of water, ice and silica as 2,090, 4,182 and 830 J / kg°C, respectively. Therefore, the heat capacity of unfrozen silica sand was 1,700 J / kg·K and that of frozen silica sand was 1,300 J / kg·K.

4.2 Freezing time and energy consumption ratio

The freeze time and the energy consumption for both freezing the specimen and maintaining the frozen state, which were estimated by the theoretical model, are summarized in Table 5. Because the chamber experiments for liquid air (Case 3 and 4) were performed in winter, the freezing time and energy consumption show a favorable result compared to the cases of liquid nitrogen.

Fig. 10 compares the theoretical estimation with the measured freezing time in the lab-scale chamber experiment. The freezing time was slightly underestimated for the cases of using liquid nitrogen while it was slightly overestimated for the cases of using liquid air due to the different room temperatures during each chamber experiment (see Table 3). It can be concluded that the theoretical model considered in this paper well describes the freezing process of the soil and can be used to design the freezing time.

In the real application of artificial ground freezing, it is necessary not only to freeze a target area, but also to maintain the frozen state for a while in order to continue a subsequent construction process. For example, in subsea tunnel construction, the frozen state should be maintained during excavation and installation of lining systems. This requires the continuous supply of energy after freezing the ground. In Table 5, the energy consumption ratio (energy consumption for maintaining the frozen state to the energy consumption for freezing soil specimens) is estimated from the theoretical model and compared for the four experimental cases. It can be seen that the energy consumption ratio is noticeably affected by external temperature. The comparable values presented in Table 5 shows the applicability of liquid air as a potential alternative refrigerant for ground freezing.

4. Conclusions

This paper presents the applicability of liquid air as a potential refrigerant for the application of artificial ground freezing. Based on the chamber experiment and the theoretical model, the following conclusions can be drawn:

- Liquid air produced under three mixing ratios in the devised laboratory equipment revealed that the standard of oxygen content in Korea (19.0 ~ 23.0 %) was achieved at the initial mixing ratio of 80 (liquid nitrogen): 20 (liquid oxygen). The final oxygen content of the produced liquid air was not affected by pressure in the cylinder or the flow rate of liquid air, but slightly higher than the initial oxygen content in the three mixing ratios.
- In the freezing chamber test to verify the application of liquid air as a freezing refrigerant, it is noted that the higher thermal conductivity of frozen soil saturated with salty water can enhance heat transfer to reduce freezing time.
- The theoretical model of heat flow well describes the freezing process of the soil, and can be used to design the freezing time. The energy consumption ratio is an important factor to calculate the total amount of energy required for maintaining frozen state, which is greatly affected by external temperature.

Acknowledgments

This research was supported partially by a grant (Project number: 13SCIP-B066321-01 (Development of Key Subsea Tunnelling Technology)) from Korea Agency for Infrastructure Technology Advancement funded by Ministry of Land, Infrastructure and Transport of Korean government and by a grant (2019R1A2C2086647) from National Research Foundation of Korea (NRF) funded by the Ministry of Education.

References

Andersland, O.B., and Ladanyi, B. (2004), *Frozen Ground*

Engineering, 2nd Edition, John Wiley & Sons, Inc., Hoboken, New Jersey, U.S.A.

Backer, L., and Blindheim, O.T. (1999), "The Oslofjord subsea road tunnel-crossing of a weakness zone under high water pressure by freezing", *Proceedings of the World Tunnel Congress 99*, Oslo, Norway, May.

Cai, H., Li, P., and Wu, Z. (2020), "Model test of liquid nitrogen freezing-temperature field of improved plastic freezing pipe", *J. Cold Reg. Eng.*, **34**(1). https://doi.org/10.1061/(ASCE)CR.1943-5495.0000204.

Colombo, G., Lunardi, P., Cavagna, B., Cassani, G., and Manassero, V. (2008). "The artificial ground freezing technique application for the Naples underground", *Proceedings of the Word Tunnel Congress 2008*, Agra, India, September.

Evirgen, B., and Tuncan, M. (2019), "A physical soil freezing model for laboratory applications", *Cold Reg. Sci. Technol.*, **159**, 29-39. https://doi.org/10.1016/j.coldregions.2018.12.005.

Gallavresi, F. (1981), "Ground freezing—The application of the mixed method (brine—liquid nitrogen)", *Eng. Geol.*, **18**(1-4), 361-375. https://doi.org/10.1016/0013-7952(81)90074-0.

Giancoli, D.C. (1984), *General Physics*, Prentice-Hall, Englewood Cliffs, New Jersey, U.S.A.

Haβ, H., and Schäfers, P. (2005), "Application of ground freezing for underground construction in soft ground", *Proceedings of the 5th international conference of TC 28 of the ISSMGE*, Amsterdam, The Netherlands, June.

Harris, J.S. (1995), *Ground Freezing in Practice*, Thomas Telford, London, U.K.

Heijboer, J., Van Den Hoonaard, J., and van de Linde, W. (2003), *The Westerschelde Tunnel: Approaching Limits,* A.A. Balkema Publishers, Lisse, The Netherlands.

Itoh, J., Lee, Y.S., Yoo, S.W., and Lee, S.D. (2005), "Ground freezing improvement for TBM maintenance in Singapore", *Proceedings of the International World Tunnel Congress and the 31st ITA General Assembly*, Istanbul, Turkey, May.

Li, D.W., Fan, J.H., and Wang, R.H. (2011), "Research on visco-elastic-plastic creep model of artificially frozen soil under high confining pressures", *Cold Reg. Sci. Technol.*, **65**(2), 219-225. https://doi.org/10.1016/j.coldregions.2010.08.006.

Mauro, A., Normino, G., Cavuoto, F., Marotta, P., and Massarotti, N. (2020), "Modeling artificial ground freezing for construction of two tunnels of a metro station in Napoli (Italy)", *Energies*, **13**(5), 1272. https://doi.org/10.3390/en13051272.

Pimentel, E., Papakonstantinou, S., and Anagnostou, G. (2011), "Case studies of artificial ground freezing simulations for urban tunnels", *Proceedings of the Word Tunnel Congress 2011 on Underground spaces in the service of a sustainable society*, Helsinki, Finland, May.

Pimentel, E., Papakonstantinou, S., and Anagnostou, G. (2012), "Numerical interpretation of temperature distributions from three ground freezing applications in urban tunnelling", *Tunn. Undergr. Sp. Tech.*, **28**, 57-69. https://doi.org/10.1016/j.tust.2011.09.005.

Saarelainen, S., Korkiala-Tanttu, L., and Viitala, J. (2004), "Railway tunnelling in frozen ground on Bothniabana", *Proceedings of the Fifth International Conference on Case Histories in Geotechnical Engineering*, New York, U.S.A., April.

Stoss, K. and Valk, J. (1979), "Uses and limitations of ground freezing with liquid nitrogen", *Develop. Geotech. Eng.*, **26**, 485-494. https://doi.org/10.1016/B978-0-444-41782-4.50041-5.

Vitel, M., Rouabhi, A., Tijani, M. and Guérin, F. (2015), "Modeling heat transfer between a freeze pipe and the surrounding ground during artificial ground freezing activities", *Comput. Geotech.*, **63**, 99-111. https://doi.org/10.1016/j.compgeo.2014.08.004.

Wang, S., Qi, J., Yu, F. and Liu, F. (2016), "A novel modeling of settlement of foundations in permafrost regions", *Geomech. Eng.*, **10**(2), 225-245. https://doi.org/10.12989/gae.2016.10.2.225.

Wang, S., Wang, Q., Qi, J. and Liu, F. (2018), "Experimental study on freezing point of saline soft clay after freeze-thaw cycling", *Geomech. Eng.*, **15**(4), 997-1004. https://doi.org/10.12989/gae.2018.15.4.997.

Wang, S., Wang, Q., Xu, J., Ding, J., Qi, J., Yang, Y. and Liu, F. (2019), "Thaw consolidation behavior of frozen soft clay with calcium chloride", *Geomech. Eng.*, **18**(2), 189-203. https://doi.org/10.12989/gae.2019.18.2.189.

Yang, Y., Lai, Y. and Chang, X. (2010), "Laboratory and theoretical investigations on the deformation and strength behaviors of artificial frozen soil", *Cold Reg. Sci. Technol.*, **64**(1), 39-45. https://doi.org/10.1016/j.coldregions.2010.07.003.

Yang, Y., Lai, Y., Dong, Y. and Li, S. (2010), "The strength criterion and elastoplastic constitutive model of frozen soil under high confining pressures", *Cold Reg. Sci. Technol.*, **60**(2), 154-160. https://doi.org/10.1016/j.coldregions.2009.09.001.

Zhang, D., Fang, Q. and Lou, H. (2014), "Grouting techniques for the unfavorable geological conditions of Xiang'an subsea tunnel in China", *J. Rock Mech. Geotech. Eng.*, **6**(5), 438-446. https://doi.org/10.1016/j.jrmge.2014.07.005.

GC